Structure, shape and dynamics of biological membranes.

Idema, T.

CHAPTER 6

MEMBRANE MEDIATED SORTING

Inclusions in biological membranes may communicate via deformations they induce on the shape of that very membrane, a purely physical effect which is not dependent on any specific interactions. In this chapter we show that this type of interactions can organize membrane domains and proteins and hence may be significant in biological systems. Using a simple analytical model we predict that membrane inclusions sort according to the curvature they impose. We verify this prediction by both numerical simulations and by comparison to experimental observations of membrane domains in phase separated vesicles.

6.1 Introduction

In the previous chapter we studied forces between membrane inclusions mediated by the membrane itself. These forces operate on the mesoscopic scale, *i.e.*, their range is comparable to the size of a cell. Membrane mediated interactions may therefore play a role in cellular organization, alongside several well known other forces, such as hydrophobic, electrostatic and Van der Waals interactions [12]. Hydrophobic forces are responsible for creating the lipid bilayer membrane in the first place, as well as for including (trans)membrane proteins (which, like lipids, have both hydrophilic and hydrophobic parts) in it. Many highly specific protein-protein interactions are a consequence of electrostatics, which are indeed crucial to the functioning of most enzymes. However, for neutral or screened inclusions electrostatic interactions do not have long range effects, which means that long range order in the membrane stems from either Van der Waals or membrane mediated interactions. Since the first decays faster ($1/r^6$) than the second ($1/r^4$), we expect the dominant contribution to be due to forces mediated by the membrane curvature. These interactions have therefore attracted the interest of several groups over recent years [97–104]. Based on these results and the quantification of membrane mediated forces in chapter 5, we demonstrate in this chapter how membrane mediated interactions give rise to long range order in a biomimetic system. In the membranes of living cells a similar breaking of the homogeneity, by the formation of patterns and long-range order, carries significant biological implications for processes like signaling, chemotaxis, exocytosis and cell division.

We study the effect of membrane mediated interactions on domain organization and pattern formation in the same experimental system that we used in chapter 5. We consider the situation that we have many relatively small L_o domains on a vesicle with a L_d background. The domains are in a metastable, kinetically arrested state, which means they have partially budded out and no longer fuse. However, they are by no means static, but rather mobile, and reorganize continuously. Because larger domains exert a greater force on their neighbors (see section 5.4), the domains will collectively try to find a configuration in which larger domains have a larger effective area around them. We expect that, due to this size-dependent interaction, the domains demix by size to achieve an optimal configuration.

We note that this membrane mediated sorting effect is different from depletion interaction in the sense that the interaction we consider here is both long ranged and soft, whereas depletion is an effect seen in systems with hard-core repulsions. Moreover, the sorting effect occurs in a system with a continuous, polydisperse particle size distribution (see figure 5.3), severely limiting the depletion effect. Depletion may of course still play a small role, but can be ignored in comparison to the membrane mediated interactions discussed here.

In this chapter we present a simple model in which we analyze the possi-

ble distributions of domains on phase separated vesicles, and find that they exhibit a striking tendency to sort. We complement this model by performing both Monte Carlo and Brownian dynamics simulations using the membrane parameters we obtained from the shape and fluctuation fits in chapter 4. The simulations give the optimal domain distribution and show the sorting effect. We find that sorting is an unavoidable consequence of the size-dependent nature of the interactions and the finite area available on a vesicle. In addition, we compare with experimental results on phase separated, ternary vesicles, which do indeed show the sorting effect. In particular, we find a correlation between the size of a domain and the size of its neighbors, which is reproduced by our simulations.

6.2 Analytical model

A somewhat oversimplified analysis of the total energy of a fully mixed and a fully demixed system gives us a direct clue as to whether the domains segregate into regions of identical-sized ones or not. Because the bending rigidity of the L_o domains is much higher than that of the L_d background (see chapter 4), we assume the domains to be rigid inclusions, as in chapter 5. The pairwise repulsive interaction potential is therefore again given by [97]

$$V \sim \frac{\alpha^2 + \beta^2}{r^4}, \tag{6.1}$$

where α and β are the contact angles of the two inclusions or rigid domains (see figure 5.5; a derivation of (6.1) is given in appendix 5.C). Although the interactions are not pairwise additive, the qualitative dependence of V on the contact angles and inclusion distance does not change if more inclusions are added to the system [99]. It is therefore possible to use a mean-field description for a finite, closed system with many inclusions, from which the prefactor in equation (6.1) can be determined experimentally (see chapter 5). Moreover, we can write effective pairwise interactions for nearest-neighbor domains, as a function of their sizes and the distance between them.

For simplicity we look at a system with only two sizes of domains, which we will call big and small for convenience. In our model the most abundant experimental domain size (with a typical radius of $3.0\ \mu\mathrm{m}$, see figure 5.3) corresponds to the small domains. For the big domains we take a radius of $(3.0\ \mu\mathrm{m}) \cdot \sqrt{2} = 4.3\ \mu\mathrm{m}$, which means that their area is twice that of the small domains.

Let us denote the number of domains by N, the number of big domains by $N_b = \gamma N$ and that of small domains by $N_s = N - N_b = (1-\gamma)N$. Likewise we denote the contact angle of a big domain by α_b, that of a small domain by α_s, and the average contact angle of a domain's nearest neighbors (in

the mean-field approach) by β. If we neglect the small curvature of the background sphere, which has surface area A, we can associate an effective radius to each domain corresponding to the patch of area which it dominates (*i.e.*, in which it is the closest domain). In a completely mixed system the effective radius of all domains is equal and given by

$$R_{\text{eff}} = \sqrt{\frac{A}{\pi N}}. \tag{6.2}$$

In a fully mixed system each of the domains has $6 \cdot \gamma$ big and $6 \cdot (1-\gamma)$ small neighbors, which allows us to calculate the potential of that configuration in the mean field approach:

$$V_{\text{mixed}} = \frac{6}{16} N_b \frac{\alpha_b^2 + \beta^2}{A^2/(\pi^2 N^2)} + \frac{6}{16} N_s \frac{\alpha_s^2 + \beta^2}{A^2/(\pi^2 N^2)} \tag{6.3}$$

where $\beta = \gamma\alpha_b + (1-\gamma)\alpha_s$. In the fully demixed system, the big domains can take up a larger fraction ϕ of the vesicle surface than they occupy in the fully mixed system. By doing so they can increase the distance between them, reducing the interaction energy. The penalty for this reduction is a denser packing of the small domains, but since their repulsive forces are smaller, the total configuration energy can be smaller than in the mixed system. We consider the regions in which we have big and small domains separately and get two effective radii:

$$R^b_{\text{eff}} = \sqrt{\frac{\phi A}{\pi N_b}}, \tag{6.4}$$

$$R^s_{\text{eff}} = \sqrt{\frac{(1-\phi)A}{\pi N_s}}. \tag{6.5}$$

For the potential energy we obtain

$$V_{\text{demixed}} = \frac{6}{16} N_b \frac{2\alpha_b^2}{(\phi A/(\pi N_b))^2} + \frac{6}{16} N_s \frac{2\alpha_s^2}{((1-\phi)A/(\pi N_s))^2}, \tag{6.6}$$

where we have assumed the number of domains is large enough that ignoring the boundary between the two regions is justified. For a fully mixed system we would have $\phi = \gamma$, *i.e.*, the area fraction assigned to the big domains is equal to their number fraction. In the demixed system the parameter ϕ becomes freely adjustable and can be tuned to minimize the interaction energy. Comparing the demixed potential (6.6) to the mixed potential (6.3), we find

$$\begin{aligned} \frac{V_{\text{demixed}}}{V_{\text{mixed}}} &= 2\left[\frac{\gamma^3}{\phi^2}\left(\frac{\alpha_b}{\alpha_s}\right)^2 + \frac{(1-\gamma)^3}{(1-\phi)^2}\right] \\ &\quad \cdot\left[\gamma(1+\gamma)\left(\frac{\alpha_b}{\alpha_s}\right)^2 + 2\gamma(1-\gamma)\left(\frac{\alpha_b}{\alpha_s}\right) + (1-\gamma)(2-\gamma)\right]^{-1}. \end{aligned} \tag{6.7}$$

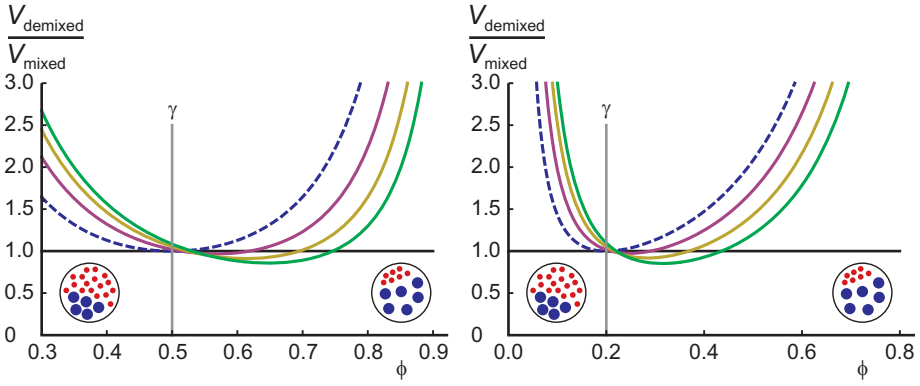

Figure 6.1: Comparison of the potential energies of the completely mixed and completely demixed state of a vesicle with domains of two different sizes. The freely adjustable parameter ϕ denotes the fraction of the vesicle's surface area claimed by the big domains. The top figure has $\gamma = \frac{1}{2}$ (equal numbers of big and small domains), and the bottom figure has $\gamma = \frac{1}{5}$ (one fifth of the domains is big). The dashed blue line indicates the case in which the big and small domains are equal in size (and hence have equal contact angles). The solid red, yellow and green lines indicate contact angle ratios α_b/α_s of 1.5, 2.0 and 2.5 respectively. Domain demixing occurs for any value of ϕ for which the potential ratio is less than 1 (black horizontal line). For comparison the number fraction γ of the big domains is indicated by the gray vertical line. Insets: typical distributions of domains for small (left) and big (right) values of ϕ. For small ϕ, the big domains are packed closely together and the small domains claim the largest area fraction, for large ϕ the situation is reversed.

Plots for several values of the parameters are given in figure 6.1. For a range of values of the adjustable parameter ϕ the energy of the demixed state is smaller than that of the mixed state; this effect becomes more pronounced as the difference in contact angle (and therefore repulsive force) increases. In the configuration which has the lowest total energy the area fraction ϕ claimed by the big domains is indeed larger than their number fraction γ.

6.3 Simulations

In the analytical model we only considered the two extreme configurations of a completely mixed and a completely demixed system. In order to be able to study also intermediate states of the system we performed Monte Carlo simulations in which we included all nearest-neighbor interactions. In these

simulations we again studied a binary system consisting of small and big domains, where the surface area of the big domains is twice that of the small ones. Starting from a random configuration of big and small L_o domains on a L_d sphere, we used Monte Carlo steps to find the energy minimum, and consistently found demixing. A typical example of a relaxation process and a configuration after 50,000 timesteps are shown in figure 6.2. The potential we used in the simulations is based on (6.1) and given by $V = V_{ij}/r^4$, with $i = 1$ for a small domain and $i = 2$ for a big one, and likewise for j. The V_{ij} values we obtained from the spring constant measurements described in chapter 5.

Complementing the Monte Carlo simulations, we also performed Brownian dynamics simulations. In these simulations, we calculate in each time step the force on each domain due to its nearest neighbors and displace it accordingly. Moreover, we add thermal fluctuations by displacing each domain a distance x over an angle θ in each timestep. The angles are sampled from a uniform distribution and the distances are sampled from the distribution $P(x) \sim \exp\left(-\frac{kx^2}{2k_BT}\right)$, where k is the effective spring constant due to the potential created by a domain's nearest neighbors (see section 5.4). In the simulations we use $k = 1.5\ k_BT/\mu\mathrm{m}^2$, corresponding to the mean value found experimentally (see figure 5.9. In the Brownian dynamics simulations, we do not just study a binary system but also a system with a more realistic exponential distribution of domain sizes (figure 5.3). Including multiple domain sizes allows for better comparison with experiment; in particular we can look for correlations between the size of a domain and its nearest neighbors. The Brownian dynamics simulations showed demixing like the Monte Carlo simulations did. An example of an obtained correlation plot is shown in figure 6.3a.

6.4 Experimental verification

Our theoretical prediction that domains segregate into regions of equal-sized ones is confirmed by experimental observations. In experiments detailed in appendix 4.A, we studied the distribution of budded domains on the entire vesicle. The vesicles we observed were lying on top of other vesicles, preventing distortion due to adhesion to the underlying coverslip. We consistently found that vesicles have regions where some domain sizes are overrepresented. An example of such an experiment is given in figure 6.3b, where two sides of the same vesicle are shown. Quantitatively we found that there is a correlation between the size of a domain and the average size of its nearest neighbors (also shown in figure 6.3b). The domain sorting occurred consistently in all 21 vesicles with budded domains we studied.

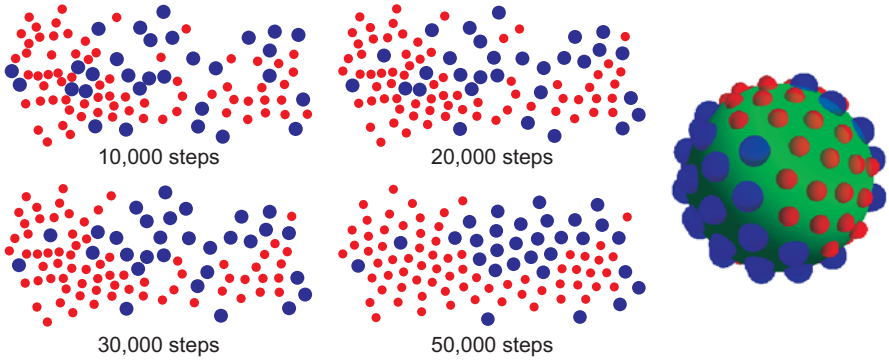

Figure 6.2: Monte Carlo relaxation of a random configuration of 70 small (red) and 30 big (blue) domains on a spherical vesicle. Left: a folded-open view of the entire vesicle, with the azimuthal angle along the horizontal direction and the polar angle along the vertical direction. The configuration is shown after 10,000 (top left), 20,000 (top right), 30,000 (bottom left) and 50,000 (bottom right) timesteps. Here $V_{12} = 3.3V_{11}$, $V_{22} = 4.5V_{11}$ and $k_{\text{B}}T = 0.25V_{11}$. Right: the configuration on a sphere after 50,000 timesteps.

6.5 Conclusion

As we have shown in this chapter, membrane mediated interactions on closed vesicles lead to the sorting of domains by size. Our analysis shows that this is due to the fact that larger domains impose a larger curvature on their surrounding membrane. We expect the same sorting effect to occur for other curvature inducing membrane inclusions, in particular cone shaped (trans)membrane proteins. This spontaneous sorting mechanism could potentially be used to create polarized soft particles. Moreover, similar sorting effects may occur in the membranes of living systems without the need of a specific interaction or an actively driven process.

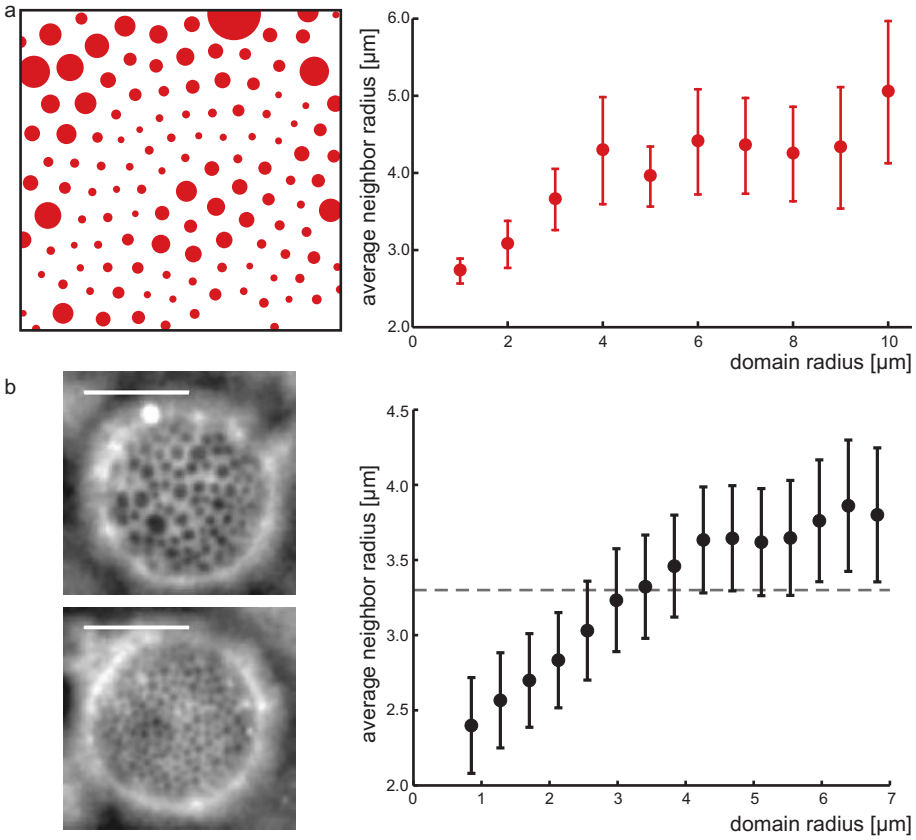

Figure 6.3: Correlations between the size of a domain and that of its nearest neighbors. (a) Results of the Brownian dynamics simulations. Left: example of the actual distribution of domains on the vesicle after 10,000 steps. Right: average correlation plot of ten Brownian dynamics simulations. Each simulation starts with 200 domains of $1.0\ \mu\mathrm{m}$ diameter. The force between two domains scales with the distance between them as $1/r^5$. The spring constant we used for the random displacements is $1.5\ k_{\mathrm{B}}T/\mu\mathrm{m}^2$. (b) Experimental data. Left: two sides of the same vesicle showing very different domain sizes; scalebar $20\ \mu\mathrm{m}$. Right: correlation plot averaged over 21 experimental vesicles; the dashed line corresponds to the average $3.3\ \mu\mathrm{m}$. Domain sizes are grouped in equally sized bins.